

Entropy Generation in a Boundary Layer Transitioning Under the Influence of Freestream Turbulence

Edmond J. Walsh

Stokes Research Institute,
University of Limerick,
Limerick, Ireland
e-mail: Edmond.Walsh@ul.ie

Donald M. Mc Eligot

Stokes Research Institute,
University of Limerick,
Limerick, Ireland;
Mechanical Engineering Department,
University of Idaho,
Idaho Falls, Idaho 83402;
Aero. Mech. Engineering Department,
University of Arizona,
Tucson, Arizona 85721

Luca Brandt

Phillip Schlatter

Linne Flow Centre,
KTH Mechanics,
SE-100, 44 Stockholm, Sweden

The objective of the present research is to develop new fundamental knowledge of the entropy generation process in laminar flow with significant fluctuations (called pre-transition) and during transition prematurely induced by strong freestream turbulence (bypass transition). Results of direct numerical simulations are employed. In the pre-transitional boundary layer, the perturbations by the streaky structures modify the mean velocity profile and induce a “quasi-turbulent” contribution to indirect dissipation. Application of classical laminar theory leads to underprediction of the entropy generated. In the transition region the pointwise entropy generation rate $(S''')^+$ initially increases near the wall and then decreases to correspond to the distribution predicted for a fully-turbulent boundary layer as the flow progresses downstream. In contrast to a developed turbulent flow, the term for turbulent convection in the turbulence kinetic energy balance is significant and can play an important role in some regions of the transitioning boundary layer. More turbulent energy is produced than dissipated and the excess is convected downstream as the boundary layer grows. Since it is difficult to measure and predict true turbulent dissipation rates (and hence, entropy generation rates) exactly other than by expensive direct numerical simulations, a motivation for this research is to evaluate approximate methods for possible use in experiments and design. These new results demonstrate that an approximate technique, used by many investigators, overestimates the dissipation coefficient C_d by up to seventeen per cent. For better predictions and measurements, an integral approach accounting for the important turbulent energy flux is proposed and validated for the case studied. [DOI: 10.1115/1.4004093]

1 Introduction

A key to improving efficiency—and thereby increasing energy sustainability and reducing fuel consumption, greenhouse gases and/or waste—is the minimization of entropy generation [1–4]. Accordingly, the overall technical aim of the present program is to develop fundamental understanding of the entropy generation process in characteristic wall shear flows. For entropy generation by fluid friction, the rates are reasonably predictable for pure laminar flows without significant fluctuations and for developed turbulent flows [5–8]. The main difficulty now lies in prediction for flows undergoing so-called “bypass” transition from laminar to turbulent states (i.e., transition prematurely induced by strong freestream turbulence). Therefore the specific *objective* of the present research is to develop new fundamental knowledge of the entropy generation process in laminar flow with significant fluctuations (called pre-transition) and during bypass transition.

One *motivation* for this research also is to evaluate approximate methods for possible use in experiments and design since it is difficult to measure and predict true turbulent dissipation rates (and hence, entropy generation rates) exactly other than by expensive direct numerical simulations. Available experimental measurements lack details and resolution necessary to determine the entropy generation rate adequately for bypass transition, particularly in the near-wall region where it is concentrated.

Recent literature on the topic of entropy generation in wall-bounded flows has been reviewed by Naterer and Camberos [4], the present authors [5,6,9] and others. To determine the pointwise entropy generation rate $S'''(x, y, z)$ completely in flows with turbulence or unsteady motion requires evaluation of the instantaneous values of the tensor $(\partial u_i / \partial x_j)$ as given by Kock and Herwig [10]. This quantity is generally not available from Reynolds-averaged Navier-Stokes (RANS) code predictions and is difficult, if not impractical, to measure directly with accuracy where it is most important. A number of investigators have used a simpler *approximation* [11–15] which corresponds to a suggestion by Rotta (Eq. (23.8d) in the Schlichting text [16]). It is equivalent to approximating the “indirect entropy generation” (turbulent dissipation) by the production of turbulence kinetic energy and, consequently, “only” requires determination of the streamwise mean velocity $U(y)$ and Reynolds shear stress $-\rho \bar{u}v(y)$ profiles. McEligot et al. [5] showed this approximation gave reasonable predictions of overall entropy generation rates for developed turbulent boundary layers but yields incorrect details near the wall. Whether or not this approximate approach can do as well for transitional boundary layers is a *question* to be answered by the present study.

Morkovin [17] denoted the situation in boundary layers where freestream turbulence of more than one per cent leads to rapid transition, bypassing the classic Tollmien-Schlichting scenario, as “bypass transition.” It is characterized by the appearance inside the boundary layer of streamwise elongated “streaks” of alternating high and low velocities relative to the mean flow, apparently first identified by Klebanoff [18–21]. As the streaks grow downstream, they undergo wavy motions which precede the breakdown into regions of intense randomized flow, turbulent spots. The spots grow in size and merge until the flow is fully turbulent. In the case where the boundary layer is subjected to significant freestream turbulence, it has been documented that the laminar boundary layer exhibits increased wall shear

Contributed by the Fluids Engineering Division of ASME for publication in the JOURNAL OF FLUIDS ENGINEERING. Manuscript received October 8, 2010; final manuscript received April 20, 2011; published online June 16, 2011. Assoc. Editor: Paul Durbin.

The United States Government retains, and by accepting the article for publication, the publisher acknowledges that the United States Government retains, a non-exclusive, paid-up, irrevocable, worldwide license to publish or reproduce the published form of this work, or allow others to do so, for United States Government purposes.

stress [22] and a significant level of fluctuations or perturbations [23–25]. These variations in laminar flow character are not treated by either the Blasius or Pohlhausen analyses of laminar flows.

Despite extensive studies over the last seven or more decades on laminar, transitional and turbulent boundary layer flows and on effects of freestream turbulence (e.g., Bradshaw [26]; Schlichting [16]; Narasimha [27]; Suder, O'Brien and Reshotko [28]; Mayle [29]; Ames and Plesniak [30]; Wang, Goldstein and Olson [31]; Jacobs and Durbin [32]; Matsubara and Alfredsson [33]; Volino, Schultz and Pratt [34]; Brandt, Schlatter and Henningson [35]; Schlatter et al. [36]; etc.), few have considered the entropy generation involved. Further, the experimental studies have lacked the measurements needed to deduce the entropy generation in the region near the wall where it is concentrated. Walsh and colleagues at the University of Limerick have pioneered the prediction and measurement of local entropy generation rate in transitional boundary layers with streamwise pressure gradients [37]. They found considerable differences between the approximate data for S''' and predictions for laminar, transitional and turbulent regions, partly due to difficulties in prediction for the transition region.

Useful insight into the problems of predicting transitional and turbulent flow by computational fluid dynamics (CFD) techniques is provided by the compendium of Launder and Sandham [38]. The state-of-the-art has been summarized well by Savill [39–41] and has been updated in various recent numerical studies (e.g., Lardeau, Li and Leschziner [42]; Walters and Cokljat [43]; Turner and Prosser [44]; etc.). Many of the studies have compared their predictions to the extensive ERCOFTAC experiments at Rolls Royce [22,45] which were conducted with hot wire anemometry in a wind tunnel and, in the transition region, typically provided mean statistics for Reynolds stresses other than the streamwise component only away from the immediate vicinity of the wall. These experiments do not provide the data needed to evaluate entropy generation by its exact definition in bypass transition.

The flow considered is unheated, incompressible and two-dimensional in the mean sense with zero streamwise pressure gradient. The present study extends the earlier research by McEligot et al. [5]. Nolan et al. [46] and Brandt, Schlatter and Henningson [35] to develop new fundamental knowledge of the entropy generation process in pre-transitional laminar flow and during bypass transition (i.e., our objective). This information has not been available previously in adequate detail. The predictions are based on the direct numerical simulation (DNS) of Brandt, Schlatter and Henningson [35]. First, key relations for evaluating entropy generation rates and intermittency are presented in the following subsections as well as discussion of the DNS treatment and some pertinent results for the example treated. Section 2 provides the evolution of the balance terms in the transport of turbulence kinetic energy (TKE) that are helpful in understanding the development of entropy generation rates S''' in bypass transition and then examines the predictions of $S''' \{x,y\}$ in the pre-transitional laminar and transitional boundary layers. Since the entropy generation rate per unit surface area S'' is useful in fluids design, Sec. 3 treats its evolution and studies its possible approximate prediction when DNS results are not available. We then summarize with some concluding remarks, including recommendation of an improved approximation approach.

2 Background

For *steady*, pure laminar two-dimensional flows under boundary layer approximations and without significant fluctuations, the pointwise entropy generation rate S''' can be expressed as

$$TS''' \{y\} = \mu \Phi \approx \mu (\partial U / \partial y)^2 \quad (1)$$

where Φ refers to the dissipation. The non-parallel effects are of the order $1/\text{Re}$ and can be considered small for the DNS results

employed herein. For a laminar boundary layer with zero pressure gradient and *negligible* fluctuations, $(S''')^+ = [f'' \{ \eta \} / f'' \{ 0 \}]^2$ where $(S''')^+$ is $(\text{Ti} S''') / (\rho u_\tau^4)$, η is the Blasius parameter $y(U_\infty / (\nu x))^{1/2}$ and $f' \{ \eta \}$ is defined as $U \{ \eta \} / U_\infty$. The function $f'' \{ \eta \}$ is available from tabulations of the Blasius solution, such as Table 7.1 by Schlichting [16].

In a flow with *fluctuations*, the time-mean value of dissipation at a point may be expanded to $\mu \Phi + \rho \varepsilon$ where the first term represents viscous dissipation of mean-flow kinetic energy (termed “viscous,” “direct” or “mean” dissipation) as above and the latter term represents dissipation of turbulent kinetic energy into thermal energy (also referred to as “indirect” or turbulent dissipation) and may be expressed as [47]

$$\rho \varepsilon = 2\mu \left[\overline{\left(\frac{\partial u}{\partial x} \right)^2} + \overline{\left(\frac{\partial v}{\partial y} \right)^2} + \overline{\left(\frac{\partial w}{\partial z} \right)^2} \right] + \mu \left[\overline{\left(\frac{\partial u}{\partial y} + \frac{\partial v}{\partial x} \right)^2} + \overline{\left(\frac{\partial v}{\partial z} + \frac{\partial w}{\partial y} \right)^2} + \overline{\left(\frac{\partial w}{\partial x} + \frac{\partial u}{\partial z} \right)^2} \right] \quad (2)$$

(This indirect dissipation is *not* the ε of popular k - ε turbulence models [48,49]). We will generally refer to $\mu \Phi$ as the viscous contribution or viscous entropy generation rate and to $\rho \varepsilon$ as the turbulent contribution. When expressed in standard wall units, the *time-mean* pointwise, total entropy generation rate for an unheated two-dimensional flow can be written as

$$(S'' \{y^+\})^+ = \left(\frac{\partial U^+}{\partial y^+} \right)^2 + \left(\frac{\partial V^+}{\partial x^+} \right)^2 + 2 \left[\left(\frac{\partial U^+}{\partial x^+} \right)^2 + \left(\frac{\partial V^+}{\partial y^+} \right)^2 \right] + \varepsilon^+ \quad (3)$$

where the indirect dissipation ε^+ is $\nu \varepsilon / u_\tau^4$

As mentioned above, by application of boundary layer and other approximations, Rotta (Eq. (23.8d), Schlichting [16]) has suggested that total dissipation in a turbulent boundary layer may be evaluated as

$$\mu \Phi + \rho \varepsilon \approx [\tau_{\text{visc}} + \tau_{\text{turb}}] (\partial U / \partial y) \approx [\mu (\partial U / \partial y) - \rho \bar{u} \bar{v}] (\partial U / \partial y) \quad (4)$$

so that the approximate volumetric entropy generation rate can be estimated as

$$(S''_{ap})^+ \approx \left[\frac{\partial U^+}{\partial y^+} + (\bar{u} \bar{v})^+ \right] \frac{\partial U^+}{\partial y^+} \quad (5)$$

In the present study we refer to use of this assumption as the *approximate* technique, as indicated by the subscript. One sees his turbulent dissipation term to be equivalent to the main contributor to production of turbulent kinetic energy. While the approximation that production is equal to turbulent dissipation may be reasonable in the typical logarithmic layer of a turbulent boundary layer beyond $y^+ \approx 30$, it has been shown by McEligot et al. [5] that they can differ significantly in the viscous layer (e.g., see Fig. 7(a) of Ref. [5]). Near the wall, production is negligible whereas turbulent dissipation is significant so there – and at the boundary layer edge — use of Eq. (5) is inappropriate.

Emmons [50] was the first to propose the concept of an intermittent transitional boundary layer. The *intermittency*, γ , is a logical function which provides a measure of the time the flow at a single point is turbulent. For $\gamma = 0$ the flow is fully laminar and conversely, if $\gamma = 1$, the flow is fully turbulent while for a value of $\gamma = 0.5$ the flow is in a transitional state with laminar and turbulent flow each existing for fifty per cent of the time. Emmons hypothesized that the transition region may be considered as a superposition of laminar and turbulent states weighted by a local intermittency level. This approach leads to a linear combination model expressed as

$$f = f_L (1 - \gamma) + f_T (\gamma) \quad (6)$$

where f represents some boundary layer quantity and subscripts L and T represent the laminar and turbulent states, respectively. Various investigators determine or define the start of transition and intermittency in various ways. Liepmann [51] used a surface tube and later observations of a hot wire signal on an oscilloscope; in the latter case, the first appearance of large sudden velocity fluctuations close to the plate — the so-called turbulent bursts — was taken as the indication of transition. Suder, O'Brien and Reshotko [28] examined five definitions: (1) distortion of mean velocity profiles, (2) change of shape factor, (3) divergence of skin friction coefficient, (4) amplitude of rms velocity fluctuation u' and (5) intermittency observed with a wall sensor. Alternatively, one may use a threshold of turbulence kinetic energy as an indicator. Fransson, Matsubara and Alfredsson [52] define a “transitional Reynolds number” to be that where $\gamma_y = 0.5$ at $(y/\delta^*) = 1.4$ and choose the values of $\gamma_y = 0.1$ and 0.9 to define where transition starts and ends, respectively. Unfortunately, not all investigators specify their definitions of transition or its precursors. Many arbitrarily identify a “start” of transition and “end” of transition by comparison to the predicted local skin friction coefficients for developed laminar and turbulent boundary layers. An “apparent” intermittency may then be calculated as $\gamma_f = (C_f - C_{f,lam}) / (C_{f,turb} - C_{f,lam})$ with C_f being the measured skin friction coefficient. The start of transition is then defined as the position where γ is first observed to be greater than zero and the end is taken as the location where it becomes unity. Comparable results may be obtained by using the measured shape factor H as the indicator. In the present study we examine use of a pointwise value as by Fransson, Matsubara and Alfredsson and a value from skin friction comparisons, say γ_y and γ_f , respectively.

3 Direct Numerical Simulation

From DNS results it is possible to obtain all terms required to calculate the direct and indirect entropy generation rates in laminar and turbulent flows exactly. Moreover, the tensor involved can be evaluated directly at each time step from the velocity field and then can be averaged in time and spanwise direction to provide a direct measure of the total entropy generation rate at a given streamwise, wall-normal position. In the current paper, for these purposes we employ results from the DNS calculations of Brandt, Schlatter and Henningson [35,36] for bypass transition. The results employed in this paper are those of their Case Four, where a pseudo-spectral code, thus with spectral accuracy, is used to solve the three-dimensional time-dependent incompressible Navier-Stokes equations over a flat plate.

A description of the code is provided by Chevalier et al. [53]. The algorithm is similar to that of Kim, Moin and Moser [54], i.e., Fourier representation in the streamwise and spanwise directions and Chebyshev polynomials in the wall-normal direction, together with a pseudo-spectral treatment of the nonlinear terms. The time advancement used is a four-step low-storage third-order Runge-Kutta method for the nonlinear terms and a second-order Crank-Nicolson method for the linear terms. Aliasing errors from the evaluation of the nonlinear terms are removed by the 3/2 rule when the FFTs are calculated in the wall-parallel plane. In the wall-normal direction it was found more convenient to increase the resolution rather than using dealiasing. The direct numerical simulations were performed according to classic guidelines in terms of resolution of a fully turbulent flow in wall units in the three spatial directions (see Brandt, Schlatter and Henningson [35] for further details); a decay of energy of at least four decades is observed in the energy spectra. The method for generation of freestream turbulence is similar to that of Jacobs and Durbin [32] with the turbulent flow described as a superposition of modes of the continuous spectrum of the linearized Orr-Sommerfeld and Squire operators.

To account correctly for the downstream growth of the boundary layer, a spatial technique is necessary. This requirement is combined with periodic boundary conditions in the streamwise direction by adding fringe regions upstream and downstream, similar to that described by Bertolotti, Herbert and Spalart [55]. The

desired in- and out-flow velocity vectors may vary with the three spatial coordinates and time. Upstream, the vector is smoothly changed from the laminar boundary layer profile at the beginning of the fringe region to the prescribed inflow velocity vector at $x = 0$, the beginning of the reported results. This vector is normally a laminar boundary layer profile, but it may also contain desired inflow disturbances: the free-stream turbulence in this case.

All quantities are non-dimensionalized using the constant freestream velocity U_∞ , ν and the displacement thickness at the nominal inlet δ_{o^*} ($x = 0$). For example, for the remainder of this paper the quantity x generally will represent the streamwise distance divided by δ_{o^*} . The computational Reynolds number is thus, $Re_{\delta_{o^*}} = U_\infty \delta_{o^*} / \nu$. For the undisturbed Blasius solution, the 99% boundary layer thickness δ_{99} is $2.85 \delta^*$. For Case Four, the inlet conditions are $Re_{\delta_{o^*}} = 300$, isotropic $Tu_{in} = 4.7\%$ and $\Lambda / \delta_{o^*} = 5$ where the turbulence intensity Tu is $[(u'^2 + v'^2 + w'^2)/3]^{1/2} / U_\infty$ and Λ is the integral length scale. The upstream fringe region covers $\Delta x = 90$. Pointwise intermittency γ_y is evaluated as the turbulent fraction, averaged in time, with the turbulent spots being identified by image processing filters.

For this example, Brandt, Schlatter and Henningson describe the transition process in terms of decay of freestream turbulence, $C_f\{Re_x\}$, $\delta^*\{Re_x\}$, $\theta\{Re_x\}$, $u'_{max}\{Re_x\}$, distributions of u' , v' and w' and other statistics. (However, turbulence energy balances were not provided although available in their DNS results.) For fluids engineers and to put the following study in perspective, streamwise developments of some pertinent integral parameters and intermittency are presented in Fig. 1. One sees that Re_θ , C_f and γ_f begin to diverge from the Blasius prediction for laminar flow without fluctuations essentially immediately at the start of calculations at $Re_x^{1/2} \approx 172$. From Fig. 1(a) it may be seen that the presence of fluctuations apparently induces more rapid growth of Re_θ . In Fig. 1(b) the letters “PS” refer to the correlation $C_f \approx 0.024/Re_\theta^{1/4}$, which agreed well with the turbulent boundary layer predictions of Schlatter et al. [56]. The seventh-power and Nikuradse correlations are presented by Schlichting [16] along with several others. These integral boundary layer parameters differ significantly from the Blasius solution for streamwise positions downstream after $Re_x^{0.5} \approx 250$, well before conventional definitions of “transition” location. While the magnitudes of the deviations can be expected to vary with Tu_{in} and turbulence length scale, our specific example as well as those of Roach and Brierley [22], Hernon and Walsh [24] and Ovchinnikov, Choudhari and Piomelli [57] demonstrate that they can be significant. The inflow conditions by different investigators differ so one can also expect their deviations to differ in magnitude. For example, the present DNS calculations employ an upstream fringe region so streaks are already developed in the boundary layer at the nominal inflow. On the other hand, Jacobs and Durbin [32] only have freestream modes at their start and show no immediate deviation.

In Fig. 1(c), γ_f is evaluated from the DNS predictions of C_f and Re_θ with C_f again being taken as $C_f \approx 0.024/Re_\theta^{1/4}$. The pointwise intermittency γ_y is calculated by identifying the turbulent regions by the magnitude of the spanwise velocity fluctuation w exceeding a threshold value; at each instant the boundaries of these apparent turbulent regions in a wall-parallel plane midway across the boundary layer were smoothed with a median filter and then γ_y was determined by time-averaging at each streamwise station. The first non-zero value of γ_y (0.00013), indicating detection of turbulent spots in the boundary layer, appears at $Re_x^{1/2} \approx 362$; we will refer to the flow upstream as a *pre-transitional* laminar boundary layer. By this location the effects of the fluctuations have modified the skin friction by about sixteen per cent above the Blasius prediction while Re_θ is about ten per cent greater. The minimum skin friction coefficient $C_{f,min}$, which is often used by experimentalists as an indicator of the location of *transition onset*, occurs later at $Re_x^{0.5} \approx 373$; at this position γ_f is about 0.12 while γ_y is still only about 0.0023 and $Re_\theta \approx 275$. Rapid increases of C_f and therefore γ_f begin after $C_{f,min}$ so we refer to the region downstream as the *transitional* boundary layer. By the last calculation

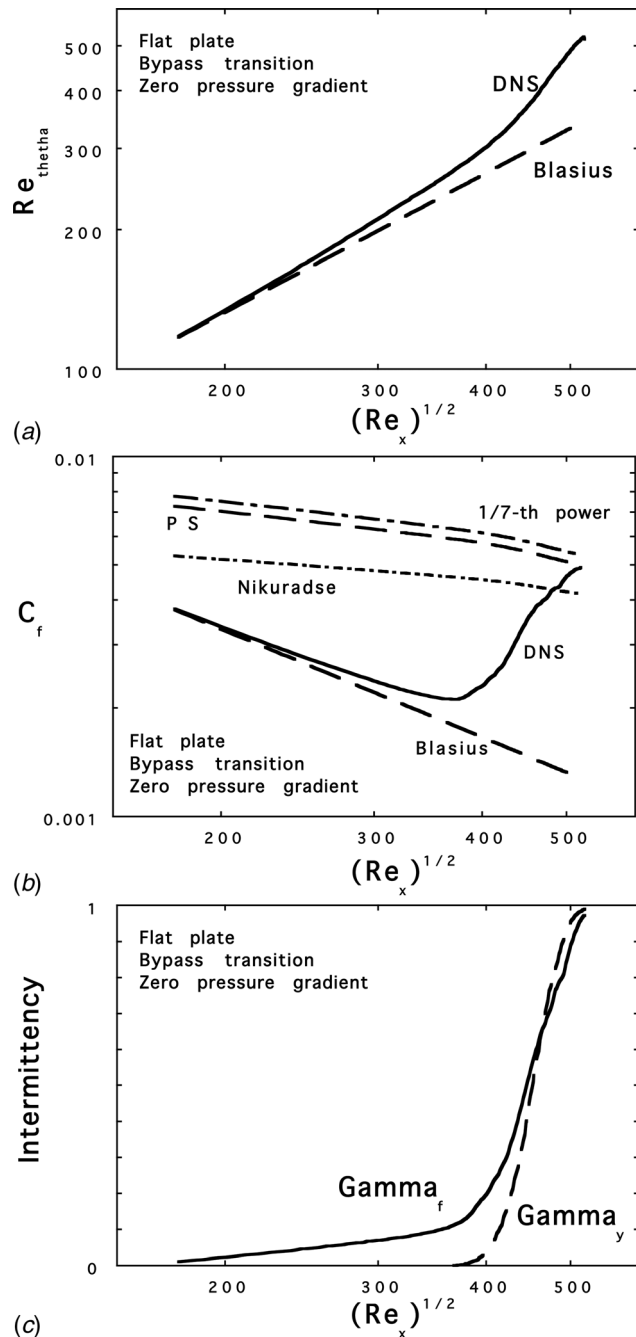


Fig. 1 Measures of evolution of the bypass transition process for the present example, $Tu_{in} = 4.7\%$ and $(\Lambda/\delta^*)_{in} = 5$; (a) Reynolds number based on momentum thickness, (b) skin friction coefficient and (c) intermittencies

position at $Re_x^{1/2} \approx 519$, the intermittencies are $\gamma_f \approx 0.97$ and $\gamma_y \approx 0.99$ so the boundary layer is nearly fully turbulent there.

Development of the streamwise mean velocity profile is demonstrated in Fig. 2. Figure 2(a) shows the effects of the perturbations on the pre-transitional laminar region as the fluctuations grow and integral parameters (Fig. 1) diverge from the theoretical behavior for a pure laminar flow without significant freestream turbulence. The location chosen, $Re_x^{1/2} \approx 350$, is slightly ahead of the detection of turbulent spots and “transition onset.” One sees that the DNS results predict slightly higher velocities than the Blasius solution near the wall and lower further out with the maximum difference of about four per cent of U_∞ occurring near $\eta = 1.5$, approximately. Measurements by Westin et al. [58] and Matsubara and Alfredsson [33] show comparable behavior. The higher

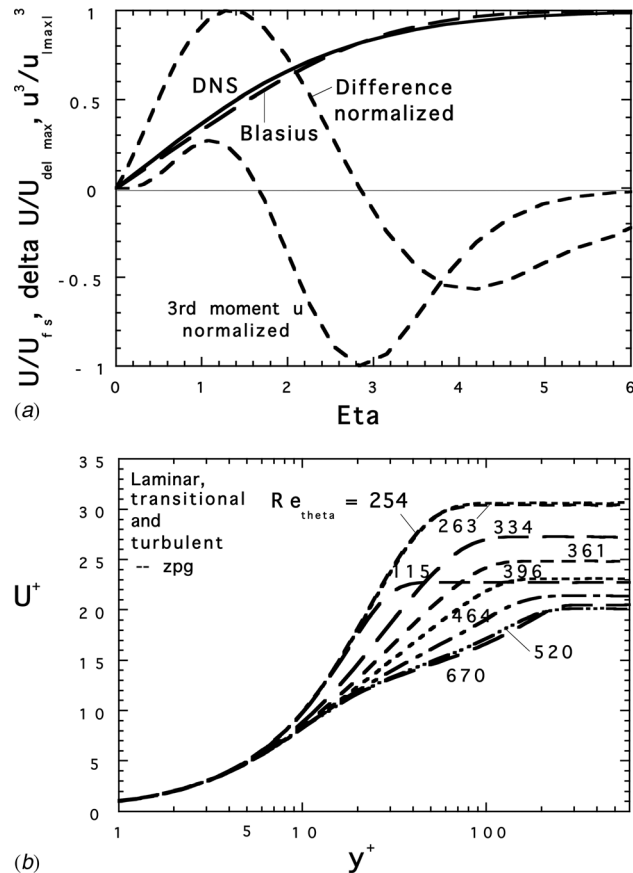


Fig. 2 Behavior of streamwise mean velocity: (a) comparison to Blasius prediction at $Re_x^{0.5} \approx 350$ ($Re_\theta \approx 254$) near the end of the pre-transitional laminar boundary layer and (b) evolution in wall coordinates

near-wall velocities correspond to higher C_f as noted by others and, as will be seen later, higher mean dissipation.

In examining measurements in a pre-transitional laminar flow with freestream turbulence of about 4.2 per cent at the leading edge, Herson, Walsh and McEligot [25] employed skewness profiles of the streamwise fluctuations to characterize the roles of positive and negative “streaky structures.” The skewness function is essentially a normalized third-moment distribution giving a measure of the lack of statistical symmetry in a signal. Accordingly, Fig. 2(a) includes the normalized profile of the third moment of u from the present DNS calculations at this location approaching transition onset (normalization is by the extreme value observed, $|-15.11|$ at $\eta \approx 2.8$). The third moment includes the fluctuating velocity cubed, and thereby retains information about the relative strength of the positive and negative fluctuations. The peak negative value represents the wall-normal location where negative fluctuations are strongest relative to the positive fluctuations. Here, the third moment demonstrates clearly that near the wall the positive streaks dominate while closer to the boundary layer edge the negative streaks are more significant. As observed by Herson, Walsh and McEligot, the absolute maximum is a negative value towards the edge of the boundary layer, indicating predominantly negative fluctuations corresponding to low-speed streaks being lifted.

Evolution to the turbulent boundary layer is presented in wall coordinates in Fig. 2(b). The first profile at $Re_\theta \approx 115$ corresponds to the initial Blasius profile in the semi-logarithmic representation. Since $U_\infty^+ = (2/C_f)^{1/2}$ by definition, the asymptotes of the profiles correspond to the variation of C_f in earlier Fig. 1(b), increasing as C_f decreases and vice versa. The last profile at $Re_\theta \approx 670$ is taken from the DNS for developed turbulent boundary layers by Schlatter et al. [56]. In the transition region the shape of the profiles

gradually evolves from that of a laminar boundary layer towards a typical turbulent wall flow with a so-called “log layer.” In an experiment for transition on a flat plate with a streamwise pressure gradient, Sharma et al. [59] found comparable trends (e.g., see Figure 9 of Ref. 59).

Of interest to experimentalists is the behavior in the immediate vicinity of the wall because the slope of the mean velocity profile can be employed to calculate the mean wall shear stress. The question is — for what distance can the curve be approximated as linear for the purpose of fitting data? If one magnifies the region of Fig. 1(b) for $y^+ < 10$ for this case (not shown), one finds that the profile is linear to within one per cent for $y^+ < \sim 6$ for the pre-transitional flow but only to $y^+ < \sim 2.6$ for the transitional region and $y^+ < \sim 3$ for the turbulent prediction. Since one cannot necessarily know the flow regime in advance, the cautious approach would be to limit such linear fitting to $y^+ < \sim 2-1/2$ or so — provided the measurements have adequate precision in this range.

4 Pointwise Entropy Generation Rate, $S'''[x, y]$

Conceptually, for S''' the indirect dissipation rate ϵ^+ could be evaluated from the turbulence kinetic energy equation, such as Eq. 8.7 by Rotta [60] (or Eq. 16.16 by Schlichting and Gersten [61]). However, many of the terms involved are difficult to measure in typical boundary layers [60,62–64], particularly in the near-wall region. This region is also where common CFD codes, using the $k-\epsilon$ model for example, are found lacking as they model the near wall flow based on empirical evidence for high Reynolds numbers and use the “pseudo”dissipation of Gersten and Herwig [48] (or the “homogeneous” dissipation of George [49]). Importantly, the near wall region is also where the majority of entropy is generated in a boundary layer [7,12,60] and therefore is the region of key interest to the designer in his attempts to understand or predict entropy generation rates. For the purposes of the present study, we use the results of DNS to calculate the terms exactly at the positions where desired.

For insight into the significance of the various terms in the turbulence kinetic energy equation during the bypass transition process and therefore, into its indirect entropy generation, the evolution of key terms is presented in Fig. 3 in wall coordinates. Numbers identify the profile locations in terms of Re_θ based on the DNS calculations. The solid lines represent profiles at the first station at $Re_x^{0.5} \approx 367$ (or $Re_\theta \approx 269$), corresponding approximately to the velocity profile in Fig. 2(a), slightly upstream of transition onset but barely after the first appearance of turbulent bursts ($\gamma_y \approx 0.0006$ here). The dashed curves are for successive locations in the transition region and then the centerline curves provide DNS predictions by Schlatter and Örlü [65] for a well-developed turbulent boundary layer at $Re_\theta \approx 3970$. The same type of dashed line represents the same streamwise location for the different terms. The scales for all subfigures are the same for easy comparison.

In general, these energy terms increase in magnitude from their pre-transitional values and then decrease, approaching the fully-turbulent predictions. In Fig. 3(a) the production term ($-\langle u_i u_j \rangle \partial U_j / \partial x_i$)⁺ is the quantity taken as the indirect or turbulent dissipation in the approximate technique (Eqs. (4) and (5)) plus the slight production from Reynolds normal stresses. The dissipation term plotted here ($-\nu \langle (\partial u_i / \partial x_i)^2 \rangle$)⁺ is the negative of the pseudo-dissipation [48] or “homogeneous” dissipation [49]; it differs slightly from the “true” dissipation (Eqs. (2) and (3)). Near the wall it is the viscous diffusion ($+\nu \partial \langle u_i (\partial u_i / \partial x_j) + [\partial u_j / \partial x_i] \rangle / \partial x_i$)⁺ which balances the turbulent dissipation. For several energy terms the maximum magnitudes for the locations shown occur at $Re_\theta \approx 361$ (or $Re_x^{0.5} \approx 441$) where the intermittency γ_y is about 35 per cent. For this location the difference between the “true” and pseudo-dissipation is typically less than two per cent of the values in the near wall region where they are largest. However, of the stations examined turbulent production,

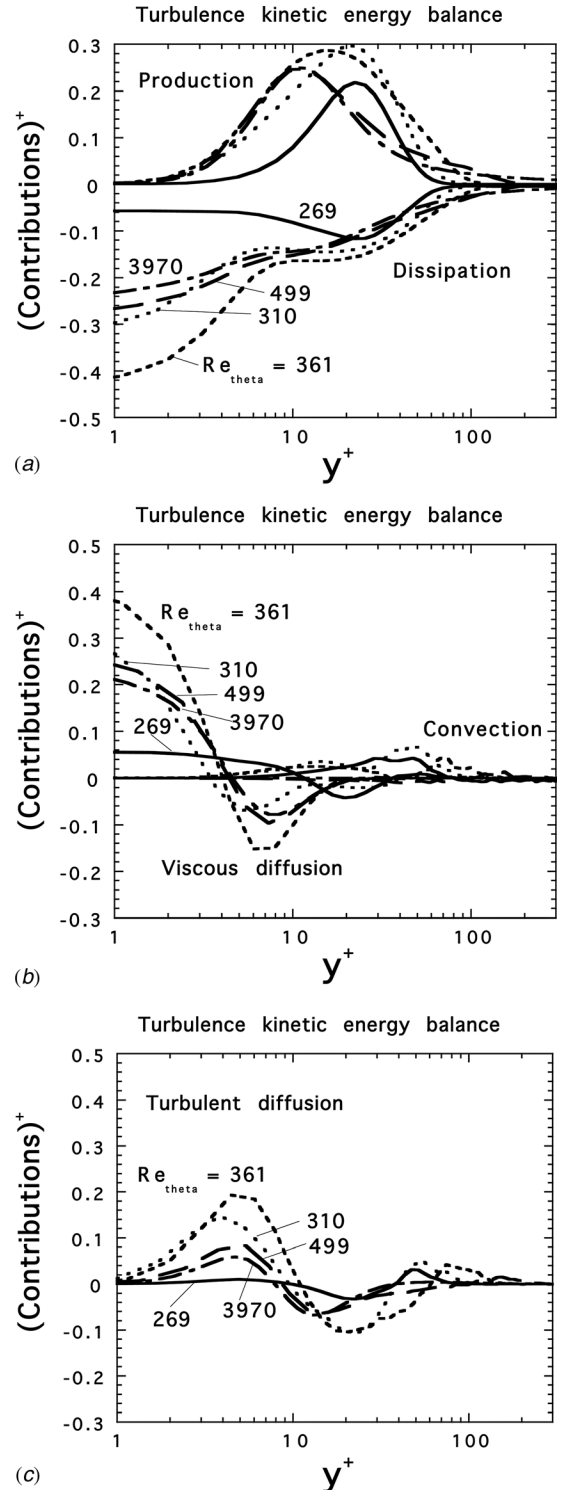


Fig. 3 Development of turbulence kinetic energy balance terms during bypass transition: (a) turbulent production and dissipation, (b) viscous diffusion and turbulent convection and (c) turbulent diffusion. All quantities are in wall coordinates

turbulent diffusion ($-\partial \langle u_j (u_i u_j / 2) \rangle / \partial x_j$)⁺ and convection ($(1/2) U_j \partial \langle (u_i u_i) \rangle / \partial x_j$)⁺ have some maxima at $Re_\theta \approx 310$ (or $Re_x^{0.5} \approx 406$) where γ_y is only about 6.1 per cent.

In contrast to the developed turbulent flow, the turbulent convection is significant – though not large – in some regions of the transitioning boundary layer. The behavior of this convection term is comparable to that predicted by the large eddy simulation

of Lardeau, Li and Leschziner [42] calculated for higher $Re_{\theta, in}$ and Tu_{in} . That is, for the developed fully-turbulent boundary layer the convection contribution can be considered negligible relative to production and dissipation terms as expected; however, it is *significant* and will be seen to play an important role for bypass transition. So-called “pressure diffusion” (not shown) peaks at a magnitude near 0.03 in the “linear” layer ($y^+ < 5$) but decreases to $O\{0.005\}$ beyond y^+ of ten so it can generally be neglected. The observations from Fig. 3 show that conventional wisdom from studies of developed boundary layers does not necessarily hold for the transitioning boundary layer.

Although the differences between absolute magnitudes of the velocities at any given location η in the *pre-transitional boundary layer* are relatively small (\approx four per cent maximum in Fig. 2(a)), the effects on the velocity-gradients-squared and therefore, the direct contribution to S''' are considerably greater. The former difference is about thirty per cent at the wall. From Fig. 2(a) one can deduce the differences in the distributions of the predicted viscous (mean) entropy generation rates across the boundary layer: near the wall the freestream turbulence results in a higher value than the Blasius case, but in the boundary layer further from the surface the opposite is the case.

The perturbations by the streaky structures contribute to the entropy generation rates and can be considered like turbulent fluctuations in a turbulent boundary layer although the term “quasi-turbulent” may be more appropriate as the origins of these perturbations are the large-scale structures [66,67]. Figure 4 shows $(S''')^+$ from the DNS in wall units, again at $Re_x^{0.5} \approx 350$. The DNS result for the total $(S''')^+$ as determined from the exact definition (Eqs. (2) and (3)) is seen to be considerably greater than the DNS viscous contribution alone, thereby illustrating the difficulty of using a predictive perspective where the streaky structures may not be modeled. (Laminar kinetic energy models as by Mayle and Schulz [23] and Lardeau, Leschziner and Li [68] attempt to account for these perturbations with varying degrees of success.) The total value calculated from Eq. (3) is termed “DNS” in the figure. The DNS viscous contribution, which is defined by the mean profile only, represents what might be calculated from single hot wire measurements, with a difference of about four per cent at the wall and about seventy per cent at $y^+ \approx 30$ ($\eta \approx 2.6$) compared to the DNS solution for the total $(S''')^+$. This difference is termed “DNS turbulent” in this figure (i.e., the difference between the DNS total and viscous results); it corresponds to ϵ^+ in Eq. (3). Although the streaks have low frequencies they lead to significant dissipation and therefore indirect entropy generation due to large gradients in the spanwise direction.

As noted in the Background section, it is often convenient or necessary to employ an *approximation* of the entropy generation rate. This approach is also evaluated in Fig. 4 via the curves labeled “approx total” for the total and “approx turbulent” for its turbulent contribution, both from the DNS results employing Eq. (5). From the comparisons of Fig. 3(a), one can see that the distributions can be expected to differ from the “exact” results, particularly at the wall where turbulent production is zero and turbulent (indirect) dissipation is about 0.1 to 0.4 in wall units. Both the “DNS turbulent” and “approx turbulent” contributions peak at $y^+ \approx 25$, corresponding to the wall-normal position where Sharma et al. [59] and others found the peak in turbulence intensity within laminar boundary layers in experiments with free-stream turbulence. Considering the approximate technique relative to the DNS exact treatment for the calculation of total $(S''')^+$, one sees that the agreement is reasonable for $15 < y^+ < 35$. This observation may be fortuitous (but it is consistent with other streamwise positions not presented here), since the fundamental assumption of turbulent production equaling dissipation locally in a laminar boundary layer with perturbations is unproven. However, from experimental and predictive perspectives the approximate approach *may provide* some opportunity to *estimate* $(S''')^+$ in pre-transitional boundary layers that contain streaky

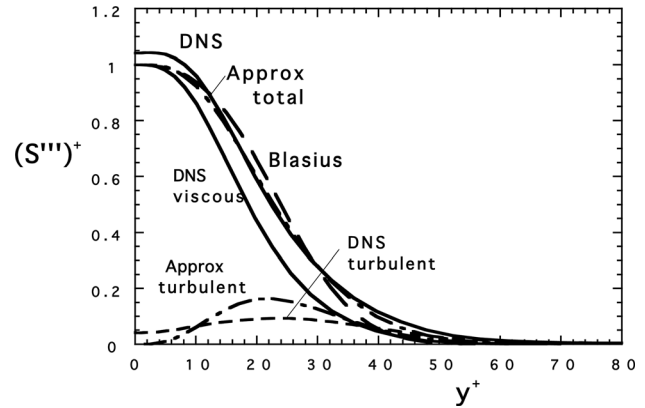


Fig. 4 Profiles of entropy generation rates in pre-transitional boundary layers at $Re_x^{0.5} \approx 350$ for $Tu_{in} = 4.7\%$ and $(\Lambda/\delta^*)_{in} = 5$ as predicted from DNS results by both exact and approximate definitions

structures induced by free stream turbulence, provided one has a measure of the equivalent Reynolds shear stress.

Development of time- and spanwise-averaged total $(S''')^+$ distributions in the wall-normal direction are shown in Fig. 5 for four streamwise locations in the *transitional region*. At $Re_x^{0.5} \approx 460$ ($Re_\theta \approx 396$), the intermittency γ_y is about 0.5 and it can be seen that $(S''')^+$ at the wall reaches its largest value. As one would expect from the behavior of the mean velocity and turbulent dissipation in Figs. 2(b) and 3(a), the entropy generation rate per unit volume approaches good agreement with the fully-turbulent DNS results of Schlatter and Örlü [65] for $Re_\theta = 3970$ as the flow develops and reaches an almost fully-developed turbulent boundary layer at $Re_x^{0.5} \approx 520$ (also $Re_\theta \approx 520$). Examination of the entropy generation rates within the turbulent spots only is desirable but beyond the scope of the present paper; however, such studies are in process at U. Limerick as demonstrated by Rehill et al. [69].

5 Energy Dissipation Coefficient, C_d

For overall design the entropy generation rate per unit area S'' is a key quantity for minimizing thermodynamic losses; it represents the lost work integrated across the boundary layer and is proportional to the areas under the curves of Figs. 4 and 5. In wall coordinates, it can be written as

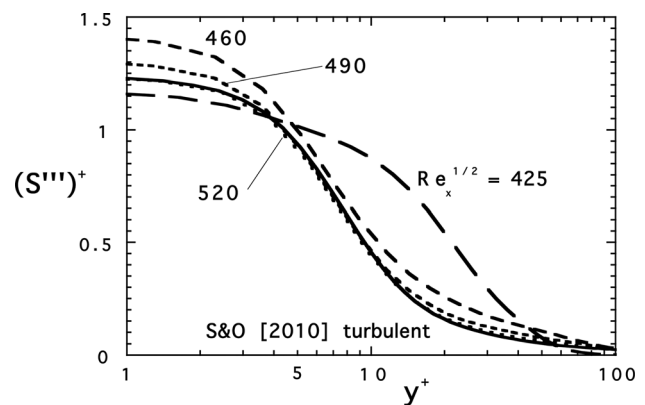


Fig. 5 Time- and spanwise-averaged total $(S''')^+$ profiles at streamwise stations ($Re_x^{0.5}$) in the transitional region, compared with the fully-turbulent DNS results of Schlatter and Örlü [65] for $Re_\theta = 3970$. Numbers indicate streamwise stations in terms of $Re_x^{0.5}$

$$(S'')^+ = \frac{TS''}{\rho U_\infty^3} = \int_0^{\delta^+} (S''' \{y^+\})^+ dy^+ \quad (7)$$

If one integrates the pointwise mean turbulence kinetic energy equation from the wall to the freestream — *subject to the presence of freestream turbulence at the edge of the boundary layer* — and adds the direct dissipation, one can derive

$$\begin{aligned} S'' \{\delta\}^+ &\approx \int_0^{\delta} (\partial U^+ / \partial y^+) dy^+ - \int_0^{\delta} (\overline{uv})^+ (\partial U^+ / \partial y^+) dy^+ \\ &- \int_0^{\delta} [(\overline{u^2})^+ - (\overline{v^2})^+] (\partial U^+ / \partial x^+) dy^+ \\ &- (d/dx^+) \int_0^{\delta} U^+ (1/2) \overline{q^2} dy^+ \\ &- (1/2) \overline{v_\delta^+ [(u_\delta^+)^2 + (v_\delta^+)^2 + (w_\delta^+)^2]} - \overline{v_\delta^+ p_\delta^+} \end{aligned} \quad (8)$$

The boundary layer thickness, δ , is defined as the wall normal position where the velocity is 99% of the free stream value, i.e., $\delta = y_{0.99U_\infty}$. Equation (8) differs from Rotta's Eq.20.22 [60] only in the additional terms for turbulent transport at the edge of the boundary layer (since fluctuations are not zero there). These last two terms represent “turbulent diffusion” and “pressure diffusion” at the edge of the boundary layer, respectively. The fourth term evolves from the convective transport of the turbulent kinetic energy by the mean flow — via the continuity equation and integration by parts; Rotta titles it “rate of turbulent energy flux.” Conceptually, all terms can be measured with particle image velocimetry, laser Doppler velocimetry and/or thermal anemometry except the pressure diffusion term. We will refer to this equation without the freestream terms (or its equivalent) as *Rotta's approach*. The first two terms, integrals of mean dissipation and production of turbulence kinetic energy by shear stress, correspond to the *approximate technique* mentioned earlier.

Jovanovic [70] has suggested that — for homogeneous turbulence — the turbulence statistics should be Gaussian and, consequently, the “mean triple products of the turbulent velocity fluctuation components” (turbulent diffusion) should become zero in the freestream. For the dissipating freestream of the *present example*, the values of the extra terms are available via the tabulations of mean statistics derived from the DNS calculations. In the freestream the values of $\overline{v_\delta^+ p_\delta^+}$ are about 0.051 or less in comparison to $(S'' \{\delta\})^+$ in a range about 17 to 26. So its contribution would be about 0.3 per cent or less, essentially negligible. The largest contribution of the freestream turbulent diffusion would be less than 1.4 per cent; however, at the location of the maximum difference between S_{exact} and S_{approx} “it would only be about 0.3 per cent. Thus, for the present case (and presumably at lower levels of freestream turbulence) the main failing of the approximate approach is neglect of the terms in Eq. (8) for turbulence energy flux. The freestream terms are small by comparison and negligible relative to the magnitude of $(S'' \{\delta\})^+$. Consequently, Rotta's integral approach should be adequate for this case.

In terms of freestream velocity, U_∞ , the entropy generation rate per unit area $(S'')^+$ may be written as a dissipation coefficient following Schlichting [16] and Denton [12] as

$$C_d = \frac{TS''}{\rho U_\infty^3} = (S'' \{\delta\})^+ (C_f/2)^{3/2} \quad (9)$$

where C_f is the skin friction coefficient and δ is the boundary layer thickness. This dissipation coefficient is often used in design so we will present these results as C_d . We compare the exact DNS predictions to Rotta's approach and the approximate technique in Fig. 6. The solid curves provide the DNS predictions for the total C_d and its viscous contribution; their difference (not shown) is the deduced turbulent contribution.

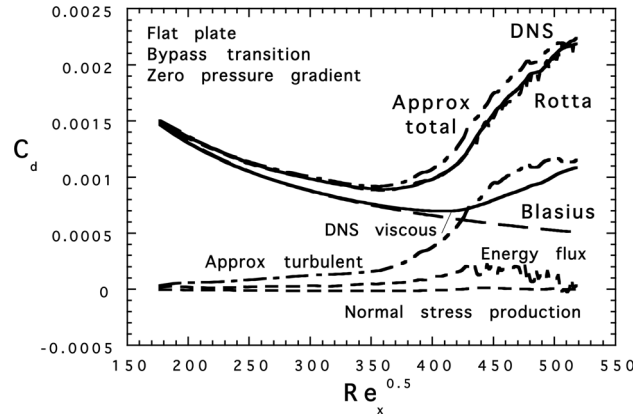


Fig. 6 Predicted dissipation coefficients C_d from exact DNS results, Rotta approach, approximate technique and Blasius solution plus individual contributions of terms in Eq. (8)

At the *beginning* of the computational domain, where $Re_{\delta^*} \approx 300$ and the velocity profile is laminar with minimal fluctuations, the Blasius and DNS solutions provide the same result for a given position since the turbulent contribution is essentially zero. Considering the viscous contribution to C_d , we saw earlier that as the flow develops the mean velocity profile deviates from the Blasius solution so C_d deviates as shown by Fig. 6; however, initially C_d is almost identical to the Blasius solution as anticipated from Fig. 1. In the *pre-transitional* boundary layer the quasi-turbulent contribution to C_d increases as the freestream turbulence initiates streaks which grow within the boundary layer, contributing about one-fifth to the total $S'' \{\delta\}$ and, hence, C_d by $Re_x^{0.5} \approx 350$. This additional lost work is not treated in any current model although it is shown here to be significant. One potential design approach to account for this increase is to use the approximate technique mentioned (if $\rho \bar{u} \bar{v}$ is known) as it shows good agreement with the DNS exact result (labeled “DNS”) for pre-transitional flow in Fig. 6. For this purpose a recent analysis by Mayle, Schulz and Bauer [71] provides a technique for the prediction of $\rho \bar{u} \bar{v}$ distributions in laminar boundary layers with freestream turbulence. Despite the large differences locally in $S''' \{\eta\}$ between the DNS and Blasius treatments seen in Fig. 4, the difference in C_d is less than two per cent at the boundary layer edge. Therefore, despite the inability of the Blasius solution to model the effects of freestream turbulence and to predict the mean velocity profile accurately, it provides a prediction for the *viscous contribution* to C_d with acceptable accuracy for most cases. When the intermittency γ_f is low the Blasius solution still predicts the viscous contribution reasonably, due to the flow being predominantly laminar. (But, as indicated earlier, the total values are higher due to the added contributions from fluctuations.) As turbulent spots grow and a higher intermittency is achieved in the downstream direction beyond $Re_x^{0.5} \approx 370$, the deviation from the Blasius solution becomes clearer.

At the *transition location* as defined by the minimum C_f ($Re_x^{0.5} \approx 375$), one sees a distinct increase in the contribution of turbulent fluctuations relative to the viscous contribution. At an intermittency γ_f of approximately 0.5 ($Re_x^{0.5} \approx 460$), the viscous and turbulent contributions appear to become the same order-of-magnitude — possibly as an artifact of averaging of the unsteady laminar and turbulent regions together rather than being physically significant. These results are believed to be related to the appearance of high-frequency secondary instabilities in the flow. The contributions of the viscous and turbulent components both remain the same order-of-magnitude as one another for the rest of the computational domain. At the end of the computation domain ($Re_\theta \approx 520$) the flow is almost fully turbulent with the viscous and turbulent contributions agreeing with the fully turbulent DNS results of Spalart [72] at $Re_\theta = 670$ to within one and five per cent, respectively.

Rotta [60] treats the terms for mean dissipation, production of TKE by Reynolds shear stress, production of TKE via the Reynolds normal stresses and convection of turbulent kinetic energy in Eq. (8) as most important for overall dissipation. These terms are shown in Fig. 6 by the curves labeled “DNS viscous,” “approx turbulent,” “normal stress production” and “energy flux,” respectively. From comparison between the curves “Rotta” and “DNS total” in Fig. 6, one can see the Rotta approach gives reasonable predictions of $C_d\{Re_x\}$.

As shown earlier concerning the TKE budget terms, the turbulent energy flux is significant through the transition region. Simply stated, more turbulent energy is produced than dissipated in the transition region and the excess is convected downstream as the transitional boundary layer grows. (The scatter in the turbulent energy flux term is probably reflective of averaging over a limited number of turbulent spots.) When the turbulent energy flux is included in integral Eq. (8), good agreement with “DNS total” is obtained. The turbulent energy flux approaches zero by the end of the domain, as expected for well-developed turbulent boundary layers where integrated production and dissipation are about equal. On the other hand, the production by Reynolds normal stresses provides a negligible contribution through the transition process—as well as in the pre-transitional and fully-turbulent regions.

The *approximate technique* is simply the sum of the mean dissipation (“DNS viscous”) and the production of turbulence kinetic energy (“approx turbulent”) and its prediction is labeled “approx total” in Fig. 6. Past $Re_x^{0.5} \approx 360$ the approximate technique predicts a significantly higher value than DNS total. In the laminar region the maximum difference is about three percent, while close to the end of the computational domain where the intermittency is high and the flow is almost completely turbulent, the difference is less than two percent. The latter observation is in agreement with the findings of McEligot et al. [5,6] for turbulent boundary layers and channel flows. In the present study our new comparisons show the maximum difference between the two techniques is about seventeen per cent and it occurs where $\gamma_y \approx 0.2$ at $Re_x^{0.5} \approx 430$ ($Re_\theta \approx 344$). Since this “usual” approximation does not predict C_d within five per cent or so, we *propose* the Rotta approach (see Rotta’s Eq. (20.22) in Ref. [60]) as better for transitional boundary layers.

The key difference between the approximate technique and the Rotta approach is inclusion of the turbulent energy flux in the latter. Thus, reasonable CFD predictions of C_d should be feasible with a transition model which predicts Reynolds shear stress and TKE – provided the transition prediction is adequate. In experiments one needs to measure the same two quantities; thermal anemometry, LDV and PIV could be used (if all three velocity components are measured) but, since the majority of the entropy generation is near the wall, spatial resolution can be a problem [73].

If one has a good prediction of the skin friction coefficient (or $\gamma_f\{Re_x\}$) and $Re_\theta\{Re_x\}$ during the transition process, one can attempt the Emmons approach [46] for design predictions. Accordingly, Fig. 7 demonstrates the application of Eq. (6) to the prediction of C_d for the present case with γ_f employed to evaluate the intermittency. The recent correlation of Walsh and McEligot [8] for fully-turbulent boundary layers at low Reynolds numbers, $C_{d,turb} \approx 0.0076/Re_\theta^{0.2}$, is used to calculate the turbulent contribution. Here the value of Re_θ is taken from the DNS results. Agreement with the DNS prediction is about four to six per cent in the transition region, better than the approximate technique over part of this range. Examination of Fig. 1(c) shows that use of γ_y for this purpose might give reasonable predictions for the approach to fully-turbulent flow but that it would be *inappropriate* for the pre-transitional boundary layer where turbulent bursts are not present to provide contributions.

6 Concluding Remarks

Since a key to improving efficiency is minimization of entropy generation and S''' is reasonably predictable for pure laminar and

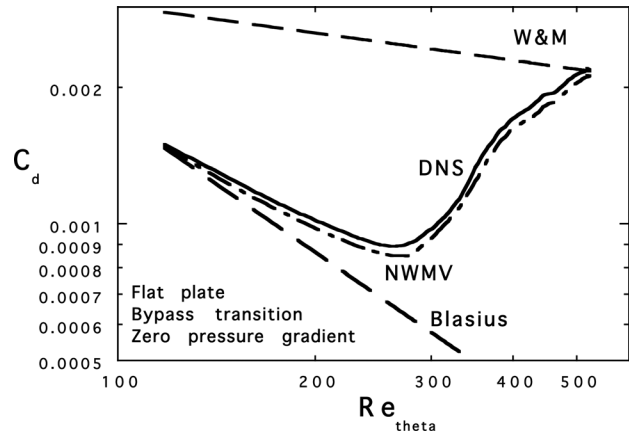


Fig. 7 Prediction of dissipation coefficient for the present example of bypass transition. NWMV = Emmons approach [46] for transitional flows and W & M = correlation of Walsh and McEligot [8] for fully-turbulent boundary layers at low Reynolds numbers

developed turbulent boundary layers, the *objective* of the present research is to develop *new* fundamental knowledge of the entropy generation process in laminar flow with significant fluctuations (called pre-transition) and during bypass transition. The DNS results of Brandt, Schlatter and Henningson [35] are employed to accomplish this objective and to examine potential design approaches. For the example studied, the inlet conditions are $Re_{\delta_0^*} = 300$, $Tu_{in} = 4.7$ per cent and $\Lambda/\delta_0^* = 5$ giving “transition onset” at $Re_x^{0.5} \approx 373$; while this case is specific, it is felt that it provides new insight into the difficulties of predicting entropy generation in boundary layers transitioning under the influence of freestream turbulence and into some potential solutions. Since it is difficult to measure and predict true turbulent dissipation rates (and hence, entropy generation rates) exactly other than by expensive direct numerical simulations, a *motivation* for this research is to evaluate approximate methods for possible use in experiments and design.

In the *pre-transitional* boundary layer, the perturbations by the streaky structures modify the mean velocity profile and cause the direct dissipation to differ from the Blasius prediction. In addition, these perturbations induce a “quasi-turbulent” contribution to indirect dissipation. The wall shear stress becomes higher and $(S''')^+$ is greater in the important wall region as well. This behavior causes the predicted entropy generation rate per unit area to diverge from the Blasius prediction gradually. The quasi-turbulent contribution amounts to about one-fifth of the total $S''\{\delta\}$ and, hence, C_d by $Re_x^{0.5} \approx 350$. Consequently, application of classical laminar theory as by Blasius and Pohlhausen will lead to under-prediction of the entropy generated in pre-transitional boundary layers with significant freestream fluctuations. Employment of a laminar kinetic energy model [23,68,71] may help but is beyond the current scope. For design purposes, if one can predict the Reynolds shear stress distribution induced by the perturbations, an improvement (which is perhaps fortuitous) can be obtained by employing a technique which approximates the indirect dissipation as equivalent to “turbulent production.”

In the *transition region* $(S''')^+$ initially increases near the wall and then decreases to correspond to the distribution predicted for a fully-turbulent boundary layer. The maximum appears near an intermittency γ_y of about 35 per cent. In contrast to a developed turbulent flow, the term for turbulent convection in the TKE balance is *significant* and can play an important role in some regions of the transitioning boundary layer. More turbulent energy is produced than dissipated in the transition region and the excess is convected downstream as the transitional boundary layer grows. In the latter part of the transition region, the indirect (turbulent)

dissipation becomes the same order-of-magnitude as the direct (mean) distribution.

These new comparisons demonstrate that the approximate technique, used by many investigators, overestimates C_d by up to seventeen per cent here. For experiments and design purposes, an integral approach developed by Rotta [60] is *proposed* and is validated for this case; it accounts for the important turbulent energy flux (the key difference between the production and dissipation of TKE) which is not treated by the approximate approach. Also for this example, the Emmons [50] linear combination model (based here on γ_f not γ_y) provided better estimates than the approximate technique in some regions.

Provided Reynolds-averaged Navier-Stokes codes can predict the transition process adequately including sensitivity to inflow turbulence length scale—which is problematical [42,43]—some may be useful in predicting entropy generation rates S''' or S'' . Since the exact calculation of indirect dissipation requires evaluation of the mean values of fluctuating-gradients-squared, an unsteady Reynolds stress model would be the minimum required. Conceptually, a “k- ϵ ” model might provide a reasonable estimate of the indirect dissipation. As noted earlier and by Bradshaw [49], the turbulent dissipation of a “k- ϵ ” model is not the ϵ of Eqs. (2) and (3). For a developed turbulent boundary layer, McEligot et al. [5] found a maximum difference of about three per cent at y^+ about five but we have not made this comparison in the present transition study. For the integral entropy generation rate S'' or C_d , to evaluate approximate equation 8 without the freestream terms would require at least a steady Reynolds stress model. However, if one neglects the production by Reynolds normal stresses, almost any k -equation model would work (again provided it can predict the transition behavior adequately).

Acknowledgment

D.M.M. thanks Professor Mark R. D. Davies, Dr. Edmond J. Walsh and their colleagues for their gracious hospitality during his summer visit to Stokes Research Institute for direct interaction. Completion of this manuscript (D.M.M.) was partly supported by the U. S. DoE Experimental Program to Stimulate Competitive Research under Grant No. DE-SC0004751 and by the Center for Advanced Energy Studies via U. S. Department of Energy Idaho Operations Office Contract DE-AC07-05ID14517. Accordingly, the U.S. Government retains a nonexclusive, royalty-free license to publish or reproduce the published form of this contribution, or allow others to do so, for U.S. Government purposes.

Nomenclature

- { } = function of
- $\langle _ \rangle$ = time and spanwise spatial average
- f = variable
- g_c = units conversion factor, e.g., 1 kg m/(N s²), 32.1739 lbm ft/(lbf s²)
- k = turbulence kinetic energy, $(\overline{u^2} + \overline{v^2} + \overline{w^2})/2$
- O{ } = order of
- p = pressure, pressure fluctuation
- q^2 = sum of velocity fluctuations squared, $(u^2 + v^2 + w^2)$
- S = entropy, entropy generation rate
- T = temperature
- U, V = mean velocity components in streamwise and wall-normal directions, respectively
- u, v, w = velocity fluctuations about means in streamwise, wall-normal and spanwise directions, respectively
- u_τ = friction velocity, $(g_c \tau_w/\rho)^{1/2}$
- \overline{uv} = mean fluctuation product in Reynolds shear stress $(-\rho \overline{uv})$
- x, y, z = coordinates in streamwise, wall-normal and spanwise directions, respectively

Non-dimensional quantities

- C_d = dissipation coefficient, $T S''/(\rho U_\infty^3)$
- C_f = skin friction coefficient, $2 g_c \tau_w/(\rho U_\infty^2)$

Re = Reynolds number; Re_{δ^*} based on displacement thickness, $U_\infty \delta^*/\nu$; Re_θ , based on momentum thickness, $U_\infty \theta/\nu$

- $(S'')^+$ = entropy generation rate per unit surface area, $TS''/(\rho u_\tau^3)$
- $(S''')^+$ = pointwise volumetric entropy generation rate, $T\nu S'''/(\rho u_\tau^4)$
- Tu = turbulence intensity, $[(\overline{u^2} + \overline{v^2} + \overline{w^2})/3]^{1/2}/U_\infty$
- U^+ = mean velocity, U/u_τ
- y^+ = wall-normal coordinate, yu_τ/ν
- δ^+ = boundary layer thickness, $\delta u_\tau/\nu$
- ϵ^+ = turbulent dissipation of turbulent kinetic energy, $\nu\epsilon/u_\tau^4$

Greek symbols

- γ = intermittency; γ_f , based on skin friction coefficient; γ_y , based on position in boundary layer
- δ = boundary layer thickness; δ^* , displacement thickness
- ϵ = dissipation of turbulence kinetic energy; ϵ_u , pseudo dissipation [48]
- η = Blasius parameter, $y (U_\infty/(\nu x))^{1/2}$
- Λ = turbulence length scale
- θ = momentum thickness
- μ = absolute viscosity
- ν = kinematic viscosity, μ/ρ
- ρ = density
- τ = shear stress; τ_w , wall shear stress
- Φ = viscous dissipation function

Superscripts

- $(_)^+$ = normalization by wall units, ν and u_τ
- $(_)'$ = root mean square value
- $(_)''$ = per unit surface area
- $(_)'''$ = per unit volume
- $(_)$ = time mean value

Subscripts

- ap = approximate
- fs = freestream value
- in = evaluated at inlet, entry
- L = laminar
- max = maximum
- o = inlet, initial value
- T = turbulent
- w = wall
- δ = boundary layer edge
- ∞ = freestream value

References

- [1] Bejan, A., 1982, *Entropy Generation Through Heat and Fluid Flow*, Wiley, New York.
- [2] Bejan, A., 1996, *Entropy Generation Minimization*, CRC, Boca Raton.
- [3] Adeyinka, O. B., and Naterer, G. F., 2004, “Modeling of Entropy Production in Turbulent Flows,” *ASME J. Fluids Eng.*, **126**, pp. 893–899.
- [4] Naterer, G. F., and Camberos, J. A., 2008, *Entropy-Based Design and Analysis of Fluids Engineering Systems*. CRC, Boca Raton.
- [5] McEligot, D. M., Walsh, E. J., Laurien, E., and Spalart, P. R., 2008, “Entropy Generation in the Viscous Parts of a Turbulent Boundary Layer,” *ASME J. Fluids Eng.*, **130**, pp. 061205-1–061205-12.
- [6] McEligot, D. M., Nolan, K., Walsh, E. J., and Laurien, E., 2008, “Effects of Pressure Gradients on Entropy Generation in the Viscous Layers of Turbulent Wall Flows,” *Int. J. Heat Mass Transfer*, **51**, pp. 1104–1114.
- [7] Walsh, E. J., and McEligot, D. M., 2008, “Relation of Entropy Generation to Wall ‘Laws’ for Turbulent Flows,” *Int. J. Comput. Fluid Dyn.*, **22**, pp. 649–657.
- [8] Walsh, E. J., and McEligot, D. M., 2009, “A New Correlation for Entropy Generation in Turbulent Shear Layers,” *Int. J. Eng. Fluid Mech*, **36**, pp. 566–572.
- [9] McEligot, D. M., Brodkey, R. S., and Eckelmann, H., 2009, “Laterally Converging Duct Flows: Part 4. Temporal Behavior in the Viscous Layer,” *J. Fluid Mech.*, **634**, pp. 433–461.
- [10] Kock, F., and Herwig, H., 2005, “Entropy Production Calculation for Turbulent Shear Flows and their Implementation into CFD Codes,” *Int. J. Heat Fluid Flow*, **26**, pp. 672–680.

- [11] Moore, J., and Moore, J. G., 1983, "Entropy Production Rates from Viscous Flow Calculations. Part I. A Turbulent Boundary Layer Flow," *ASME Paper* 83-GT-70.
- [12] Denton, J. D., 1993, "Loss Mechanisms in Turbomachines," *ASME J. Turbomach.*, **115**(4), pp. 621–656.
- [13] O'Donnell, F. K., and Davies, M. R. D., 1999, "Measurements of Turbine Blade Aerodynamic Entropy Generation Rate," *Proc., I. Mech. E., C557/055*, 3rd European Conf. Turbomachinery, Professional Engineering Publishing, London, UK, London, pp. 43–53.
- [14] Stieger, R. D., and Hodson, H. P., 2003, "Unsteady Dissipation Measurements on a Flat Plate subject to Wake Passing," *Proc., Inst. Mech. Eng., Part A*, **217**, pp. 413–419.
- [15] Hyhlik, T., and Marsik, F., 2006, "New Approach to Turbulence Model Testing based on the Entropy Production and the Analysis of Simple Wall Flows," *Turbulence, Heat and Mass Transfer 5*, K. Hanjalic, Y. Nagano and S. Jakirlic, eds., Begell House, New York, pp. 377–380.
- [16] Schlichting, H., 1968, *Boundary Layer Theory*, 6th ed., McGraw-Hill, New York.
- [17] Morkovin, M. V., 1969, "On the Many Faces of Transition," *Viscous Drag Reduction*, C. S. Wells, ed., Plenum, New York, pp. 1–31.
- [18] Klebanoff, P. S., 1971, "Effect of Freestream Turbulence on the Laminar Boundary Layer," *Bull. APS*, **10**(11), p. 1323.
- [19] Kendall, J. M., 1985, "Experimental Study of Disturbances Produced in a Pre-transitional Laminar Boundary Layer by Weak Free-stream Turbulence," *AIAA Paper* 85-1695.
- [20] Kendall, J. M., 1998, "Experiments on Boundary Layer Receptivity to Free-stream Turbulence," *AIAA Paper* 98-0530.
- [21] Schmid, P. J., and Henningson, D. S., 2001, *Stability and Transition in Shear Flows*, Springer, New York.
- [22] Roach, P. E., and Brierley, D. H., 1990, "The Influence of a Turbulent Free-stream on Zero Pressure Gradient Transitional Boundary Layer Development, Part I: Test Cases T3A & T3B," *Proc., 1st ERCOFTAC Workshop on Numerical Simulation of Unsteady Flows and Transition to Turbulence and Combustion*, O. Pironneau, W. Rodi, I. L. Ryhming, A. M. Savill and T. V. Troung, eds., Cambridge University Press, Cambridge, pp. 319–347.
- [23] Mayle, R. E., and A. Schulz, 1997, "The Path to Predicting Bypass Transition," *ASME J. Turbomach.*, **119**, pp. 405–411.
- [24] Hernon, D., and Walsh, E. J., 2007, "Enhanced Energy Dissipation Rates in Laminar Boundary Layers subjected to Elevated Levels of Free Stream Turbulence," *Fluid Dynamics Research*, **39**, pp. 305–319.
- [25] Hernon, D., Walsh, E. J., and McEligot, D. M., 2007, "Instantaneous Fluctuation Velocity and Skewness Distributions Upstream of Transition Onset," *Int. J. Heat Fluid Flow*, **28**, pp. 1272–1279.
- [26] Bradshaw, P., 1967, "The Turbulence Structure of Equilibrium Boundary Layers," *J. Fluid Mech.*, **29**, pp. 625–645.
- [27] Narasimha, R., 1985, "The Laminar-Turbulent Transition Zone in the Boundary Layer," *Prog. Aerosp. Sci.*, **22**, pp. 29–80.
- [28] Suder, K. L., O'Brien, J. E., and Reshotko, E., 1988, "Experimental Study of Bypass Transition in a Boundary Layer," *NASA Tech. Memo.* 100913.
- [29] Mayle, R. E., 1991, "The Role of Laminar-Turbulent Transition in Gas Turbine Engines," *ASME J. Turbomach.*, **113**, pp. 509–537.
- [30] Ames, F. E., and Plesniak, M. W., 1997, "The Influence of Large-scale, High-intensity Turbulence on Vane Aerodynamic Losses, Wake Growth and the Exit Turbulence Parameters," *ASME J. Turbomach.*, **119**, pp. 182–192.
- [31] Wang, H. P., Goldstein, R. J., and Olson, S. J., 1999, "Effect of High Free-stream Turbulence with Large Length Scale on Blade Heat/Mass Transfer," *ASME J. Turbomach.*, **121**, pp. 217–224.
- [32] Jacobs, R. G., and Durbin, P. A., 2001, "Simulations of Bypass Transition," *J. Fluid Mech.*, **428**, pp. 185–212.
- [33] Matsubara, M., and Alfredsson, P. H., 2001, "Disturbance Growth in Boundary Layers Subjected to Free-Stream Turbulence," *J. Fluid Mech.*, **430**, pp. 149–168.
- [34] Volino, R. J., Schultz, M. P., and Pratt, C. M., 2003, "Conditional Sampling in a Transitional Boundary Layer Under High Freestream Turbulence Conditions," *ASME J. Fluids Eng.*, **125**, pp. 28–37.
- [35] Brandt, L., Schlatter, P., and Henningson, D. S., 2004, "Transition in Boundary Layers Subject to Free-Stream Turbulence," *J. Fluid Mech.*, **517**, pp. 167–198.
- [36] Schlatter, P., Brandt, L., de Lange, H. C., and Henningson, D. S., 2008, "On Streak Breakdown in Bypass Transition," *Phys. Fluids*, **20**, pp. 101505–1–101505-15.
- [37] Walsh, E., Myose, R., and Davies, M. R. D., 2002, "A Prediction Method for the Local Entropy Generation Rate in a Transitional Boundary Layer with a Free Stream Pressure Gradient," *ASME Paper* GT-2002-30231.
- [38] Launder, B. E., and Sandham, N. D., eds., 2002, *Closure Strategies for Turbulent and Transitional Flows*, Cambridge University Press, Cambridge.
- [39] Savill, A. M., 1993, "Some Recent Progress in the Turbulence Modeling of Bypass Transition," *Near-Wall Turbulent Flows*, R. M. C. So and B. E. Launder, eds., Elsevier, New York, pp. 829–848.
- [40] Savill, A. M., 2002a, "By-Pass Transition Using Conventional Closures," *Closure Strategies for Turbulent and Transitional Flows*, B. E. Launder and N. D. Sandham, eds., Cambridge University Press, Cambridge, Ch. 17, pp. 464–492.
- [41] Savill, A. M., 2002b, "New Strategies in Modeling By-Pass Transition," *Closure Strategies for Turbulent and Transitional Flows*, B. E. Launder and N. D. Sandham, eds., Cambridge University Press, Cambridge, Ch. 18, pp. 493–521.
- [42] Lardeau, S., Li, N., and Leschziner, M. A., 2007, "Large Eddy Simulation of Transitional Boundary Layers at High Free-stream Turbulence Intensity and Implications for RANS Modeling," *ASME J. Turbomach.*, **129**, pp. 311–317.
- [43] Walters, D. K., and Cokljat, D., 2008, "A Three-Equation Eddy-Viscosity Model for Reynolds-Averaged Navier-Stokes Simulations of Transitional Flow," *ASME J. Fluids Eng.*, **130**, pp. 121401-1–121401-14.
- [44] Turner, C., and Prosser, R., 2009, "The Application of the Laminar Kinetic Energy to Turbulent Transition Prediction," *Turbulence, Heat and Mass Transfer 6*, K. Hanjalic, Y. Nagano and S. Jakirlic, eds., Begell House, New York, pp. 209–212.
- [45] Pironneau, O., Rodi, W., Ryhming, I. L., Savill, A. M., and Troung, T. V., eds., 1992, *Numerical Simulation of Unsteady Flows and Transition to Turbulence*, Cambridge University Press, Cambridge.
- [46] Nolan, K., Walsh, E. J., McEligot, D. M., and Volino, R. J., 2007, "Predicting Entropy Generation Rates in Transitional Boundary Layers Based on Intermittency," *ASME J. Turbomach.*, **129**(3), pp. 512–517.
- [47] Cebeci, T., and Bradshaw, P., 1984, *Applicational and Computational Aspects of Convective Heat Transfer*, Springer, New York.
- [48] Gersten, K., and Herwig, H., 1992, *Strömungsmechanik*, Vieweg, Braunschweig.
- [49] Bradshaw, P., 1995, "Addendum to 'A Note on Turbulent Energy Dissipation in the Viscous Near Wall Region' [Phys. Fluids A5, 3305 (1993)]," *Phys. Fluids*, **7**, p. 2297.
- [50] Emmons, H. W., 1951, "The Laminar-Turbulent Transition in a Boundary Layer," *J. Aero. Sci.*, **18**, pp. 490–498.
- [51] Liepmann, H. W., 1943, "Investigations on Laminar Boundary-Layer Stability and Transition on Curved Boundaries," *NACA Wartime Report* W-107, ACR No. 3H30.
- [52] Fransson, J. H. M., Matsubara, M., and Alfredsson, P. H., 2005, "Transition Induced by Free-Stream Turbulence," *J. Fluid Mech.*, **527**, pp. 1–25.
- [53] Chevalier, M., Schlatter, P., Lundbladh, A., and Henningson, D. S., 2007, "SIMSON: A Pseudo-spectral Solver for Incompressible Boundary Layer Flows," *Tech. Report* KTH/MEK/TR-07/07-SE, KTH Mechanics, Stockholm.
- [54] Kim, J., Moin, P., and Moser, R. D., 1987, "Turbulent Statistics in Fully Developed Channel Flow at Low Reynolds Number," *J. Fluid Mech.*, **177**, pp. 133–166.
- [55] Bertolotti, F. P., Herbert, T., and Spalart, P. R., 1992, "Linear and Nonlinear Stability of the Blasius Boundary Layer," *J. Fluid Mech.*, **242**, pp. 441–474.
- [56] Schlatter, P., Örlü, R., Li, Q., Brethouwer, G., Fransson, J. H. M., Johansson, A. V., Alfredsson, P. H., and Henningson, D. S., 2009, "Turbulent Boundary Layers up to $Re_\theta = 2500$ studied through Simulation and Experiment," *Phys. Fluids*, **21**, pp. 051702-1–051702-4.
- [57] Ovchinnikov, V., Choudhari, M. M., and Piomelli, U., 2008, "Numerical Simulations of Boundary-Layer Bypass Transition Due to High-Amplitude Free-Stream Turbulence," *J. Fluid Mech.*, **613**, pp. 135–169.
- [58] Westin, K. J. A., Boiko, A. V., Klingmann, B. G. B., Kozlov, V. V., and Alfredsson, P. H., 1994, "Experiments in a Boundary-Layer Subjected to Free-Stream Turbulence: Part I. Boundary-Layer Structure and Receptivity," *J. Fluid Mech.*, **281**, pp. 193–218.
- [59] Sharma, O. P., Wells, R. A., Schlinker, R. H., and Bailey, D. A., 1982, "Boundary Layer Development on Turbine Airfoil Suction Surfaces," *ASME J. Eng. Power*, **104**, pp. 698–706.
- [60] Rotta, J. C., 1962, "Turbulent Boundary Layers in Incompressible Flow," *Prog. Aeronaut. Sci.*, **2**, Pergamon, Oxford, pp. 1–219.
- [61] Schlichting, H., and Gersten, K., 2000, *Boundary Layer Theory*, 8th Revised and Enlarged Edition, Springer, Berlin.
- [62] Hinze, J. O., 1975, *Turbulence*, 2nd ed., McGraw-Hill, New York.
- [63] Wallace, J. M., and Foss, J., 1995, "The Measurement of Vorticity in Turbulent Flows," *Ann. Rev. Fluid Mech.*, **27**, pp. 469–514.
- [64] Elsner, J. W., and Elsner, W., 1996, "On the Measurement of Turbulence Energy Dissipation," *Meas. Sci. Technol.*, **7**(10), pp. 1334–1348.
- [65] Schlatter, P., and Örlü, R., 2010, "Assessment of Direct Numerical Simulation Data of Turbulent Boundary Layers," *J. Fluid Mech.*, **659**, pp. 116–126.
- [66] Zaki, T. A., and Durbin, P. A., 2005, "Mode Interaction and the Bypass Route to Transition," *J. Fluid Mech.*, **531**, pp. 85–111.
- [67] Zaki, T. A., and Saha, S., 2010, "On Shear Sheltering and the Structure of Vortical Modes in Single- and Two-fluid Boundary Layers," *J. Fluid Mech.*, **626**, pp. 111–147.
- [68] Lardeau, S., Leschziner, M. A., and Li, N., 2004, "Modelling Bypass Transition with Low-Reynolds-number Nonlinear Eddy-Viscosity Closure," *Flow, Turbul. Combust.*, **73**, pp. 49–76.
- [69] Rehill, B., Walsh, E. J., Nolan, K., McEligot, D. M., Brandt, L., Schlatter, P., and Henningson, D. S., 2010, "Entropy Generation Rate in Turbulent Spots in a Boundary Layer subject to Freestream Turbulence," *Seventh IUTAM Symposium on Laminar-Turbulent Transition*, P. Schlatter and D. S. Henningson, eds., Springer, Dordrecht, pp. 557–560.
- [70] Jovanovic, J., 2009, Personal communication.
- [71] Mayle, R. E., Schulz, A., and Bauer, H.-J., 2008, "Reynolds Stress Calculations for Pre-transition Boundary Layers with Turbulent Free Streams," *ASME Paper* GT2008-50109.
- [72] Spalart, P. R., 1988, "Direct Simulation of a Turbulent Boundary Layer up to $Re_\theta = 1410$," *J. Fluid Mech.*, **187**, pp. 61–98.
- [73] Vukoslavcevic, P. V., Berattis, N., Balaras, E., Wallace, J. M., and Sun, O., 2008, "On the Spatial Resolution of Velocity and Velocity Gradient-based Turbulence Statistics Measured with Multi-Sensor Hot-Wire Probes," *Exp. Fluids*, **46**, pp. 109–119.